Gas Production from Class 1 Hydrate Accumulations

*George J. Moridis and Timothy S. Collett

*Lawrence Berkeley National Laboratory, Earth Sciences Division, 1 Cyclotron Rd., Berkeley, CA 94720, U.S.A.
U.S. Geological Survey, Denver Federal Center, Box 2504 MS939, Denver, CO 80225, U.S.A.
GJMoridis@lbl.gov

Keywords: gas hydrate, production, depressurization, thermal stimulations

Abstract

Class 1 hydrate accumulations, characterized by the presence of a zone of mobile gas underneath the immobile hydrate zone, appear to be promising targets for gas production. In this paper, we discuss gas production from three deposits that cover the spectrum of Class 1 hydrate specimens. Under favorable conditions, simple depressurization appears to be an effective production strategy capable of providing large gas volumes, a large portion of which originate from hydrate dissociation. However, the necessary low operating pressures at the production wells result in lower temperatures and a progressively more difficult gas release, because of the endothermic nature of the dissociation reaction. The problem may be alleviated by coupling depressurization with thermal stimulation, leading to substantial increases in gas production resulting from the constant supply of heat to sustain dissociation. Gas production from Class 1 hydrate deposits is affected by the initial pressure and temperature conditions, the hydraulic and wettability properties of the hydrate-bearing media, the thickness of the hydrate and free gas zones, and the production-injection well system and configuration.

Introduction

Gas hydrates are solid crystalline compounds in which gas molecules are encaged inside the lattices of ice crystals. Vast amounts of hydrocarbons are trapped in hydrate deposits [Sloan, 1998]. Such deposits occur in two distinctly different geologic settings where the necessary low temperatures and high pressures exist: in the permafrost and in deep ocean sediments.

Current estimates of the worldwide quantity of hydrocarbon gas hydrates vary widely, and a range between 10^{15} to 10^{18} m^3 has been reported [1]. Note that these estimates are not the result of a systematic attempt at resource evaluation specifically focused on hydrates, but are based on data obtained largely while targeting conventional hydrocarbon resources. Even by the most conservative estimates, the total quantity of gas in hydrates may surpass, by a factor of two, the energy content of the total fuel fossil reserves recoverable by conventional methods [1]. The magnitude of this resource commands attention because it could make hydrate reservoirs a substantial future energy resource. The potential importance of hydrates is further augmented by the environmental attractiveness of gas (as opposed to solid and liquid) fuels. Although the current energy economics cannot support gas production from hydrate accumulations, their potential clearly demands further evaluation.

The three main methods of hydrate dissociation for gas production are: (1) depressurization, in which the pressure is lowered to a level lower than the hydration pressure P_H at the prevailing

temperature, (2) thermal stimulation, in which the temperature is raised above the hydration temperature T_H at the prevailing pressure, and (3) the use of inhibitors (such as salts and alcohols), which causes a shift in the P_H-T_H equilibrium through competition with the hydrate for guest and host molecules [1].

The numerical studies of gas production in this paper were conducted using the EOSHYDR2 model [2], a member of the TOUGH2 [3] family of general-purpose simulator for multicomponent, multiphase fluid and heat flow and transport in the subsurface. EOSHYDR2 models the behavior of methane-bearing binary hydrates in porous media. It can describe the nonisothermal hydrate formation and/or dissociation (equilibrium or kinetic), gas release involving any combination of the possible dissociation mechanisms, phase behavior, and fluid and heat flow under conditions typical of natural hydrate deposits.

Classification of Natural Hydrate Accumulations in Geologic Media

In terms of characteristics (which, in turn, have a strong impact on production strategies), hydrate accumulations can be divided into three main classes. Class 1 accumulations comprise two zones: the hydrate interval (often exhibiting a very low effective permeability because of large hydrate saturations in the pore space) and an underlying two-phase fluid zone with free (mobile) gas. In this class, the bottom of the hydrate stability zone (i.e., the location above which the formation of hydrates becomes possible) usually coincides with the bottom of the hydrate interval. In terms of gas production, this is the most desirable class for exploitation because of the thermodynamic proximity to the hydration equilibrium at the highest possible T_H (necessitating only small changes in pressure and temperature to induce dissociation).

Class 2 deposits feature two zones: a hydrate-bearing interval, overlying a mobile water zone with no free gas (e.g., an aquifer). Class 3 accumulations are composed of a single zone, the hydrate interval, and are characterized by the absence of an underlying zone of mobile fluids. In Classes 2 and 3, the entire hydrate interval may be well within the hydrate stability zone, and can exist under equilibrium or stable conditions. The desirability of Class 2 and 3 accumulations as gas production targets is less well defined than for Class 1 deposits, and can be a complex function of several issues, including thermodynamic proximity to hydration equilibrium, initial conditions, environmental concerns, and economic considerations [4,5].

Production from Class 2 and Class 3 hydrates has been discussed by [4] and [5]. In this paper, we focus on gas production from Class 1 hydrate deposits in permafrost formations for which field data are available. The results generally apply to ocean deposits, although boundary conditions can play a more important role in such accumulations.

Case Studies of Gas Production from Class 1 Hydrate Accumulations

Case 1: An Accumulation with Significant Potential

The schematic in Figure 1 shows gas production from a Class 1 hydrate accumulation in the North Slope of Alaska [6]. The initial conditions in the hydrate zone and in the underlying free gas zone, as well as all pertinent hydraulic and operational parameters, are listed in Figure 1. Gas is produced from five identical wells producing from the free gas zone at a cumulative rate of $Q = 4.2475 \times 10^6$ standard m^3/day (1.5×10^8 ft^3/day). This production scenario leads to depressurization-induced hydrate dissociation. The specifics of the numerical simulations involved in this study were discussed in detail in [7].

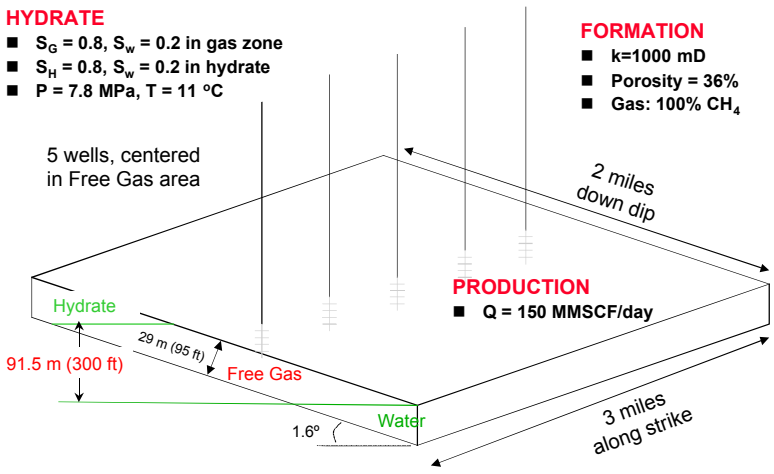

Figure 1. Gas production from the Class 1 hydrate accumulation in Case 1, North Slope, Alaska

Figure 2 shows the cumulative volumes of hydrate-originating CH_4 released during the depressurization-induced dissociation (both equilibrium and kinetic) and the cumulative gas volume produced from the system over the four-year duration of the study. A comparison of these curves provides a measure of the level of replacement of gas from the free-gas zone by CH_4 released during dissociation. Note that the kinetic study had a decidedly conservative bend, assuming large pore spaces and, consequently, low hydrate particle area in the dissociation model of Kim et al. [8] used by EOSHYDR2. Thus, the kinetic solution in Figure 2 represents the worst-case scenario and provides an estimate for the lower bound of the possible solutions, while the equilibrium solution provides the upper bound.

The results in Figure 2a indicate that, assuming an equilibrium process, dissociation can replace a large portion of the CH_4 produced from the free-gas zone. This portion can be as high as 90%, and although it declines at later times, is well above the 50% level at the end of the study period. For the reasons explained above, the gas volume released through kinetic dissociation is substantially smaller. The corresponding effects on the pressure evolution in the free-gas zone are shown in Figure 2b. Under equilibrium dissociation, the pressure decline is much milder than that for kinetic dissociation, because the free gas zone is replenished by the large CH_4 releases from the dissociating hydrate.

The results are elucidated in Figure 3, which shows the evolution over time of the rate of CH_4 release. For equilibrium dissociation, the rate increases initially because the pressure drop in the free gas zone (caused by the gas production) increases with time, leading to larger pressure differentials and, consequently, to increased depressurization-induced dissociation and larger volumes of released gas. However, the rate begins to decline after a maximum is reached at about t = 220 days. This occurs when the effect of increasing depressurization is overcome by the counteracting progressive cooling of the hydrate (due to the strongly endothermic nature of dissociation), which makes dissociation increasingly difficult. For kinetic dissociation in Figure 3(b), the CH_4 release rate shows different magnitudes but a similar pattern, characterized by a rapidly increasing initial phase, a maximum, and a declining phase.

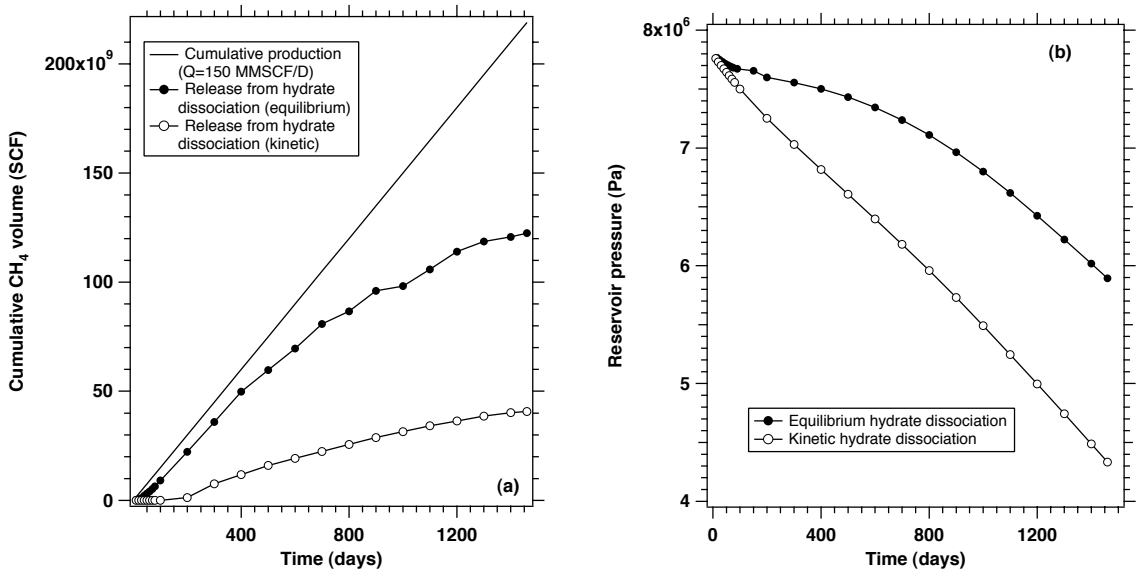

Figure 2. Cumulative release of CH_4 from hydrate dissociation (a) and pressure evolution (b) during gas production from the Class 1 hydrate in Figure 1

The geologic system in Figure 1 is a particularly appealing specimen of a Class 1 hydrate deposit, characterized by the confluence of all possible conditions favorable to enhanced gas production from hydrate dissociation. This accumulation is endowed by a thick free-gas zone (91.5 m = 300 ft), a thick hydrate zone (about 183 m = 600 ft), a very large interface area of the hydrate with the free gas, and a large intrinsic permeability (10^{-12} m^2 = 1 darcy). The bottom of the hydrate zone is at hydrate equilibrium and marks the lowest point at which hydrate occurrence is possible, i.e., the effect of the geothermal gradient exceeds that of the hydrostatic pressure. Thus, a very small perturbation of pressure or temperature is sufficient for gas dissociation to begin. The large intrinsic permeability *k* is indicative of low capillary pressures.

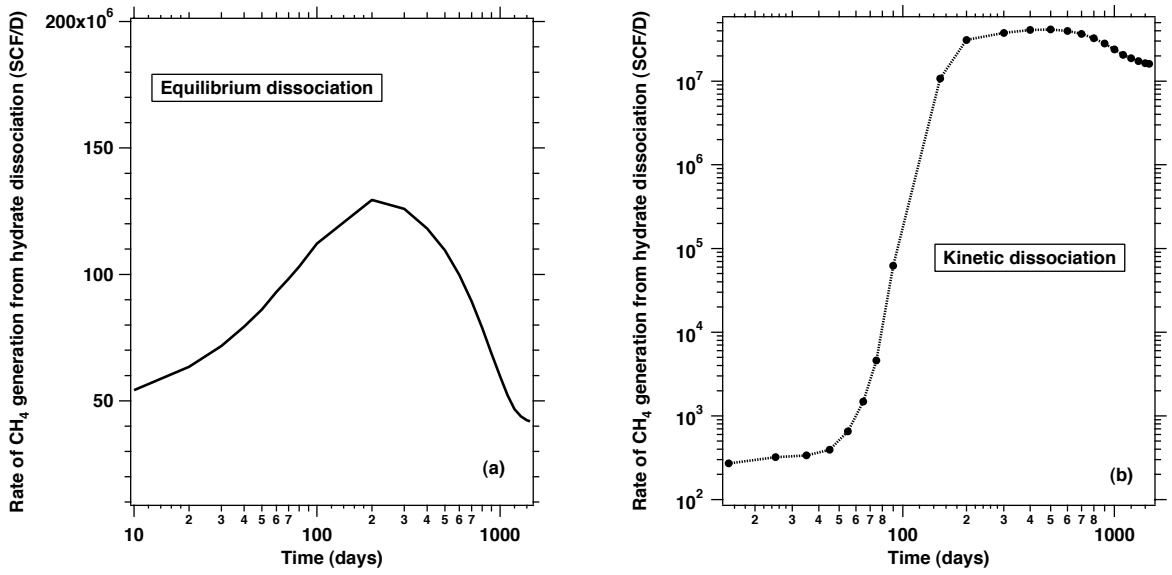

Figure 3. Release rate of CH_4 from the (a) equilibrium and (b) kinetic dissociation of the hydrate deposit in Figure 1

Coupled with the thick free gas-zone, it leads to low water saturations in the free gas zone and rapid drainage of the very large amounts of water released during dissociation. This combination of factors prevents the build-up of water saturation in the vicinity of the dissociating hydrate and alleviates the potential problem of impeded gas flows resulting from adverse relative permeability conditions. The tilted system allows concentration of the draining water near the lowest point of the formation, thus localizing water storage and limiting its adverse effects on flow.

The large k results in pressure declines that are mild and nearly uniform in the reservoir, resulting in dissociation from practically the entire interface. The mild pressure drops allow cooling to be slower and distributed over the whole interface, thus in turn allowing more effective heat transfer from the surroundings and higher overall temperatures. Such mild processes are far better in allowing the slow process of heat conduction to supply the heat necessary for dissociation than steeper pressure gradients. Steeper pressure drops may lead to an initial burst of gas release, but this is localized and self-limiting because the resulting rapid cooling can overwhelm the slow mechanism of heat conduction (the only energy source under pure depressurization), leading to progressively slower dissociation. An additional advantage of the hydrate deposit in Figure 1 is that T_H at the interface is at the highest possible level, providing a relatively large heat reservoir to fuel the endothermic dissociation.

Because of its endothermic nature, the depressurization-induced hydrate dissociation leads to a temperature decline, which, in turn, progressively limits further dissociation by shifting the T_H-P_H equilibrium (see Figure 4). If the pressure fueling dissociation is no higher than the P_H corresponding to the freezing point of water (as affected by the prevailing salinity), the hydrate saturation S_H is sufficiently high, and the hydrate temperature is low, then it is possible to experience freezing of the water and a severe reduction in gas production (because of the corresponding reduction in relative permeability). Ultimately, this leads to a complete cessation of dissociation. Thus, an important issue in this case of pure depressurization is the ability of the hydrate system to thermally recuperate within a reasonable time frame.

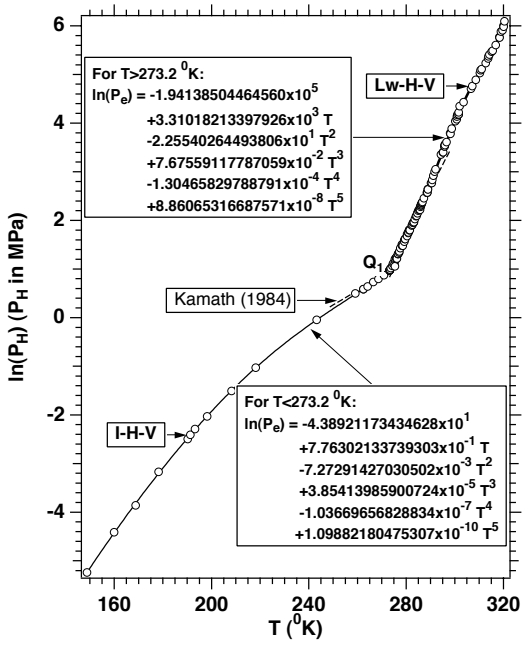

Figure 4. Pressure-temperature equilibrium of the simple methane hydrate [2]

The thermal recuperation period $t_{\Theta R}$ is defined as the time needed for the geothermal gradient (i.e., the heat flux from deeper geologic strata) to restore the hydrate system to its original temperature profile after the cessation of production. The $t_{\Theta R}$ is affected by the magnitude and rate of pressure decline, the hydrate temperature and saturation, and the thermal properties of the hydrate system. If $t_{\Theta R}$ is short, then the appeal of pure depressurization is enhanced because the practically inexhaustible deeper geothermal reservoir can provide the necessary heat to sustain dissociation. In such a case, the production strategy would involve alternating cycles of gas production (based on pure depressurization) and thermal recuperation (TR).

Figures 5(a) and 5(b) show the evolution of temperature during the $t_{\Theta R}$ of the hydrate accumulation of Case 1 (Figure 1) at the end of the four-year period of gas production from the depressurization-induced hydrate dissociation, and correspond to two different rock thermal conductivity values. Note that the EOSHYDR2 model [2] assumes thermal equilibrium and uniform thermal properties in each gridblock of the discretized domain, and employs the parallel model of Bejan et al. [10] to describe the thermal conductivity of the hydrate-bearing porous media. The temperature distribution at the end of gas production is marked by a significant decline in temperature in the vicinity of the dissociation front.

Figures 5(a) and 5(b) indicate that TR is a rather slow process, with the $t_{\Theta R} > 500$ days (at which time the temperature distribution continues to exhibit large deviations from the target of the original profile). The significant increase in the rock thermal conductivity from Figure 5(a) to 5(b) does improve the speed of thermal recovery, but the effect appears to be sublinear and does not change the overall recuperation pattern. It is noteworthy that the temperature recuperation is not uniform throughout the profile, but is localized near the region of minimum temperature at the end of the production cycle. Thus, the earliest and largest temperature increases during the TR cycle occur in the area of maximum dissociation, while other parts of the formation (such as the free gas zone) show minimal temperature increases.

The obvious conclusion drawn from Figures 5(a) and 5(b) is that TR is unlikely to be part of a practical production strategy because the $t_{\Theta R}$ exceeds realistic periods of commercial well shut-down. Consequently, long-term gas production from hydrates based on pure depressurization will have to involve higher operating pressures (i.e., lower depressurization levels and weaker dissociation-driving forces), corresponding to T_H above the freezing point of water and resulting in lower rates. Alternatively, it may be necessary to employ thermal stimulation in order to provide an alternate source of heat (to counter the adverse effects of dissociation-induced cooling) if large pressure differentials and/or large production rates are involved during depressurization.

Case 2: A Smaller-Scale System

Figure 6 depicts a Class 1 hydrate accumulation in the Eileen area of North Slope, Alaska, and corresponds to the geology and conditions in the Northwest Eileen State-2 well. The initial conditions at the bottoms of the C1 (hydrate zone) and C2 (free gas zone) units are listed on Figure 6. The deposit is confined by impermeable top and bottom boundaries, has no water-saturated zone, and has substantially thinner hydrate and free gas zones than the ones in Case 1. Because of its large areal extent at the site, the hydrate deposit behaves as an infinite system in this one-year study.

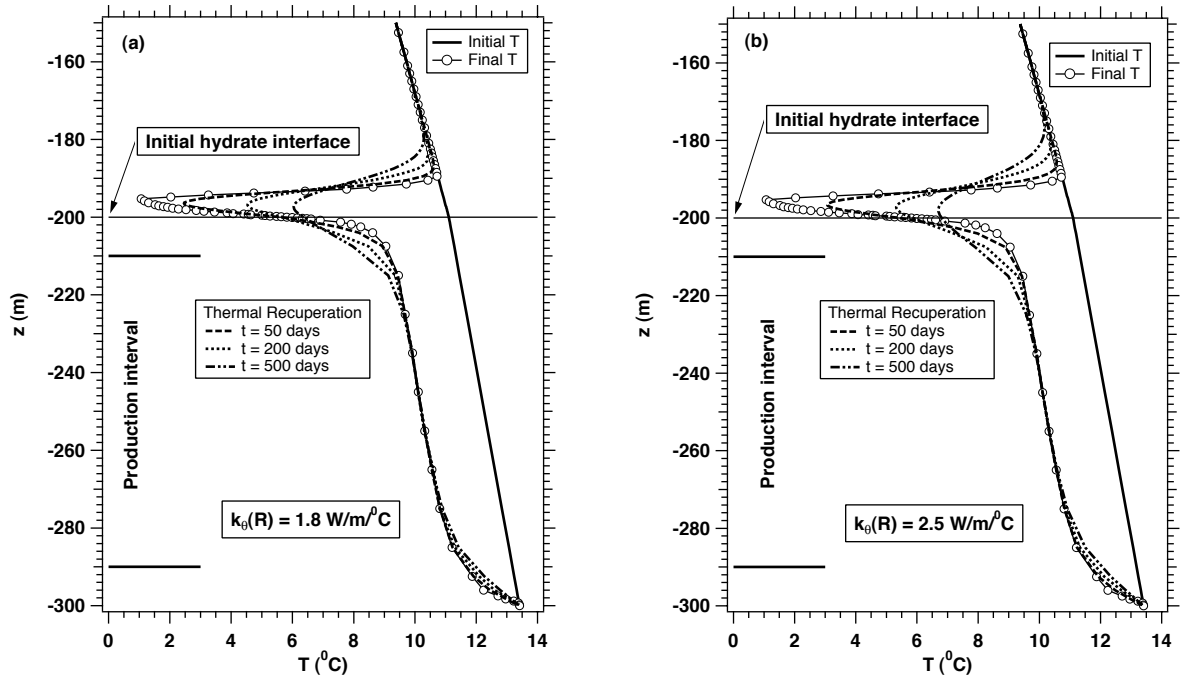

Figure 6. Temperature evolution during thermal recuperation along the axis of Well #3 after cessation of production (at t = 4 years, denoted as "final") in Case 1

Two gas production scenarios are investigated. The first involves simple depressurization from a single well and was simulated using a cylindrical grid involving 54 x 47 nonuniform gridblocks in (r,z). The second involves a combination of depressurization and thermal stimulation in a multi-well (5-spot) system, in which the distance between the production and injection wells was 50 m. A cartesian 3-D grid involving 25 x 25 x 47 gridblocks in (x,y,z) was used in this case. In either scenario, the wells were completed in the top 1.85 m (5.5 ft) of the C2 unit, and equilibrium dissociation was assumed.

Figure 7 shows the cumulative volume of dissociation-induced gas release under pure depressurization when the single production well is maintained at atmospheric pressure (i.e., at the maximum possible pressure differential). Thus, the results correspond to the upper bound of gas release. Such a production scenario is markedly different from that in Case 1, as it is expected to yield the highest dissociation rates at the early stage of production. This is supported by the evolution of gas production in Figure 8(a), which indicates that significant volumes of gas can be produced from a single well. Additionally, Figure 8(a) demonstrates that gas is by far the dominant component in the production stream, while the production of water constitutes a minuscule portion of the total fluid production. This is particularly positive because it indicates that the significant amounts of water released during dissociation drain rapidly (aided by the large intrinsic k) and do not inhibit gas flow to the well. The very large contribution of hydrates to production is demonstrated by Figure 8(b), which shows the mass fraction of gas from dissociation in the produced gas. Note, however, that the production rate and cumulative volume are significantly lower than those in Case 1, despite the similarity of the initial conditions, and of the hydraulic and thermal properties. This is attributed to the thinner hydrate and free gas zone, resulting in more rapid hydrate cooling over a larger area during dissociation.

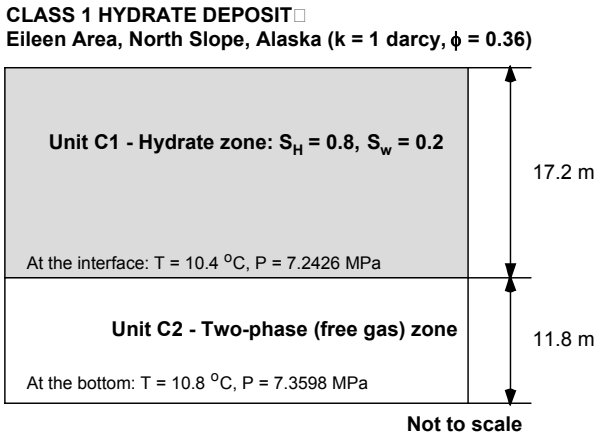

Figure 7. A schematic of the Class 1 hydrate accumulation in Case 2, Eileen Area, Alaska

Wettability issues (i.e., relative permeability k_r and capillary pressure P_c) are expected to be far more important in deposits with relatively thin hydrate and free gas intervals (such as this one). This is because a lower phase k_r limits the reach of the dissociation front, while a higher P_c hinders the drainage of water from dissociation and inhibits gas flow. The wettability effects on gas release from hydrates are demonstrated in Figure 7, which shows that a change in the wettability properties from that of sand to that of clay reduces the released gas volume by over an order a magnitude (although the intrinsic permeability remains the same). Note that the preferred wetability properties in EOSHYDR2 [2] are computed based on the model of Parker et al. [9] that uses common parameters to describe both k_r and P_c.

When depressurization is coupled with thermal stimulation, the effect on gas release is multiplicative, as indicated in Figure 9. When a 5-spot well configuration is used (with the production wells kept at atmospheric pressure, while superheated steam at a rate Q = 1.85 kg/s and an enthalpy H = 3.2 x 10^6 J/Kg is injected into the injection wells), gas release from hydrates increases by a factor of almost 5 in the 1-year duration of the study. This is possible because the buoyancy of the injected steam and the flow field (dictated by the pressure distribution in the C2 unit and in the dissociated part of the C1 unit) enhance steam contact with the dissociating hydrate interface, raising the temperature and readily supplying the heat needed for dissociation.

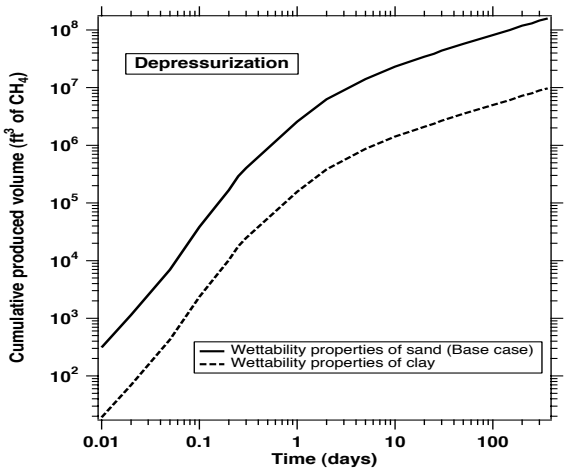

Figure 7. Depressurization-induced gas release from dissociating hydrates during production in Case 2

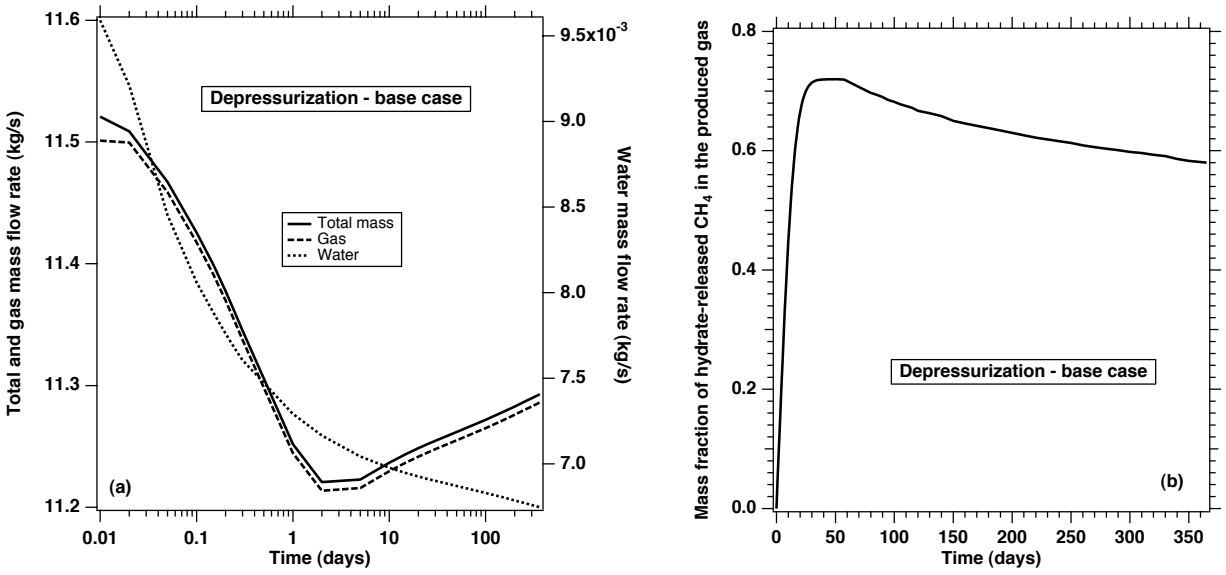

Figure 8. Phase mass flow rates (a) and gas mass fraction (b) at the producing well in Case 2

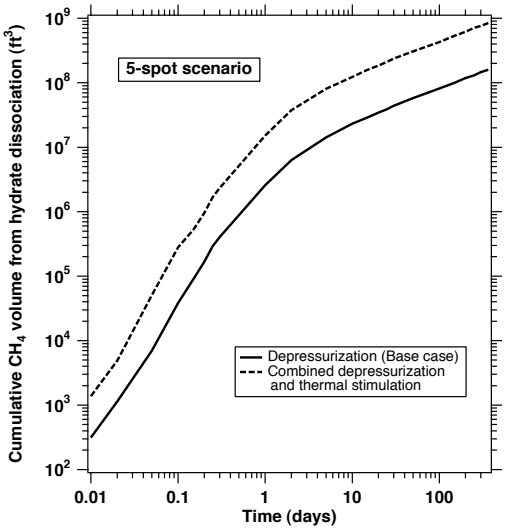

Figure 9. Gas release from hydrates in Case 2 using a combination of depressurization and thermal stimulation, and employing a 5-spot injection/production well configuration.

Case 3: Production from Challenging Class 1 Hydrate Deposits

This case addresses the low end of the spectrum of Class 1 hydrate deposits, which involve thin gas zones underlain by infinite-acting aquifers. A representative specimen is the hydrate accumulation at Mallik, Mackenzie River Delta, Northwest Territories, Canada [11], which is bounded by impermeable top and bottom strata, and involves a 20 m thick hydrate zone, a 1.5 m thick free gas zone and a 20 m thick water-saturated zone [11]. Because gas production from this type of Class 1 accumulation was extensively investigated [4], the subject will not be discussed in detail here—only a short review will be offered instead.

Unlike the Class 1 hydrates discussed in Cases 1 and 2, such deposits do not appear to be appealing candidates for depressurization-based commercial gas production because of serious water upconing problems. These lead to rapid deterioration in the gas-to-water ratio in the production stream (Figure 10a) and/or low production rates (in order to delay its onset). Note the very low production rate Q in Figure 10—necessary to sustain gas production for just a few days—and the significant mass fraction of gas from hydrates in the produced gas (Figure 10b). Note that Q=1.673x10^{-3} kg/s is the mass flow rate of total fluid withdrawal (i.e., gas and water), and corresponds to the rather minuscule volumetric flow rate of 225 standard m^3/day (about 8000 SCF/day) when only gas is produced. The upcoming problem can be reduced by using horizontal wells (Figure 10), and further alleviated if multi-well injection-production systems combining depressurization and steam-based thermal stimulation are employed [4]. Injection of a hot gas can further improve the production potential of such a deposit because it enhances the gas relative permeability while delivering heat (through buoyancy and pressure distribution) to the hydrate interface, i.e., the dissociation target [4]. While this is technically feasible, there are significant technical, safety, and economic challenges that severely limit the potential of such an approach. Moreover, even if these obstacles could be surmounted, the water upconing problem is never eliminated, and stabilization (in the case of steam or hot gas injection) of the gas-to-water ratio may be the best possible outcome [4].

If sufficiently large pressure differentials are applied, or if depressurization continues for a long time, the pressure decline can result in practically complete water saturation over a significant radius from the well, transforming the accumulation from a Class 1 to a Class 2 hydrate deposit. Strategies for gas recovery from different types of this class of hydrates have been discussed in [4] and Moridis [5].

Summary and Conclusions

This paper focuses on the study of gas production from Class 1 hydrate accumulations, i.e., deposits characterized by a hydrate zone underlain by a zone of mobile (free) gas. Three cases that cover the range of Class 1 hydrate deposits are analyzed, and the sensitivity of gas production to several important parameters is investigated.

Simple depressurization appears to be a promising production strategy in a Class 1 deposit located in the North Slope, Alaska. This deposit (Case 1) occurs in a sloping formation, with a thick free-gas zone overlain by a thick hydrate zone and underlain by an aquifer. Under these conditions, depressurization-induced dissociation of the hydrates (when assumed to be an equilibrium process) is capable of replenishing over 90% of the very substantial gas withdrawal rate of Q = 4.2475 x 10^6 standard m^3/day (1.5 x 10^8 ft^3/day) from five wells. Although it is not currently known whether dissociation is an equilibrium or a kinetic process, this study determined the bounds of the possible solutions. The high rates of dissociation and the corresponding large gas volumes originating from the hydrates are made possible by the high intrinsic permeability, the large phase-relative permeabilities, the low capillary pressures and the thick free-gas zone of the hydrate-bearing formation, which allow rapid drainage and unimpeded gas flow to the producing well. This is further enhanced by a high porosity and initial hydrate saturation, as well as by the system geometry, which allows collection of the draining water at the bottom of the sloping formation.

Figure 10. Gas mass fraction (a) and contribution of hydrate to gas production (b) at the single producing well (vertical or horizontal) in Case 3 [4]

Under pure depressurization, the low operating pressures (needed to maximize production rates) at the production wells result in hydrate cooling, leading to a progressively lower gas-release rate because of the endothermic nature of the dissociation reaction. Sufficiently low pressures and/or high production rates can even lead to water freezing and a drastic decline in gas production. Maintaining the well pressure at a level no lower than the hydration pressure corresponding to the freezing point of water can eliminate such a problem, but may be impractical because this relatively high pressure can greatly limit production. As a potential component of a production strategy, thermal recuperation, defined as the restoration of the deposit temperature to its initial level (i.e., the one prior to production) through geothermal heat fluxes from deeper formations, appears to be impractically slow and ineffective.

Depressurization-induced dissociation in the Class 1 hydrate deposit of Case 2 (also located in the North Slope, Alaska)—with relatively thin hydrate and free gas zones, and having similar properties and initial conditions—appears to produce more modest gas volumes. By coupling depressurization with thermal stimulation in a multi-well injection/production system, the combined effect is multiplicative and leads to substantial increases in gas production because of the constant supply of heat can sustain dissociation. It is noteworthy that, in Case 2, wettability issues can have a dramatic effect on gas production because of the thinner free gas zone. Additionally, a very large mass fraction of the produced gas originates from hydrate dissociation, while the mass fraction of water in the production stream is encouragingly low.

Gas production from the Class 1 hydrate deposits with very thin gas zones underlain by aquifers (Case 3) does not appear promising with standard dissociation approaches. This is because of the low rates necessitated to limit the water mass fraction in the production stream. Under these conditions, horizontal wells appear to have a slight advantage over single vertical wells. Multi-well injection/production systems employing a combination of depressurization and thermal stimulation appear to be more promising (although still insufficiently productive), and their

potential increases when using a non-condensable gas as the heating agent (an issue that may present challenges).

These observations should only be viewed as general principles and observations—because the significant variability and case sensitivity, the lack of field data, and the insufficient body of prior experience and literature on gas production from hydrates [2,5] do not allow the confidence of definitive conclusions. Thus, caution should be exercised in interpreting these results.

Acknowledgments

This work was supported by the Assistant Secretary for Fossil Energy, Office of Natural Gas and Petroleum Technology, through the National Energy Technology Laboratory, under the U.S. Department of Energy, Contract No. DE-AC03-76SF00098. Thanks are extended to Scott Digert and Robert Hunter for providing important data for the Class 1 hydrate deposit discussed in Case 1 of the paper. The authors are indebted to Timothy Kneafsey and John Apps of LBNL for their insightful review comments.

References

(1) Sloan, E.D., *Clathrate Hydrates of Natural Gases*, Marcel Dekker, Inc.: New York, NY, 1998.
(2) Moridis, G.J., Numerical Studies of Gas Production from Methane Hydrates; Society of Petroleum Engineers, SPE 75691, 2002 (in press, *SPE Journal,* 2004).
(3) Pruess, K.; Oldenburg, C.; and Moridis, G., *TOUGH2 User's Guide, Version 2.0, Report LBNL-43134*, Lawrence Berkeley National Laboratory: Berkeley, CA, 1999.
(4) Moridis, G.J.; Collett, T.S.; Dallimore, S.R.; Satoh, T.; Hancock, S.; and Weatherhill, B., *Numerical Studies of Gas Production Scenarios From Several CH_4-Hydrate Accumulations at the Mallik Site, Mackenzie Delta, Canada*, Report LBNL-50257, Lawrence Berkeley National Laboratory: Berkeley, CA, 2002 (in press, *J. Petrol. Sci. Eng.,* 2004).
(5) Moridis, G.J., Numerical Simulation Studies of Thermally-Induced Gas Production From Hydrate Accumulations With No Free Gas Zones at the Mallik Site, Mackenzie Delta, Canada; Society of Petroleum Engineers, SPE 77861, 2002 (in press, *SPE Res. Eval. Eng.,* 2004).
(6) Hunter, R.; and Digert, S.A., Personal communication, 2002.
(7) Moridis, G.J.; and Collett, T.S., *Strategies for Gas Production from Hydrate Accumulations Under Various Geological and Reservoir Conditions, Report LBNL-52568*, Lawrence Berkeley National Laboratory: Berkeley, CA, 2002.
(8) Kim, H.C.; Bishnoi, P.R.; Heideman, R.A.; and Rizvi, S.S.H, *Chem. Eng. Sci*., **1987**, *42*, 1645-1653.
(9) Parker, J.C.; Lenhard, R.J.; and Kuppusamy, T., *Water Resour. Res*., **1987**, *23(4)*, 618-624.
(10) Bejan, A., *Convection Heat Transport*, John Wiley & Sons: New York, NY, 1984.
(11) *Scientific Results from JAPEX/JNOC/GSC Mallik 2L-38 Gas Hydrate Research Well, Mackenzie Delta, Northwest Territories, Canada*; Dallimore, S.R.; Uchida, T.; and T.S. Collett, Eds., Geological Survey of Canada Bulletin 544, 1999.